



# Enrichment of mesophilic and thermophilic mixed microbial cultures for syngas biomethanation in bubble column bioreactors under continuous operation



Víctor Rodríguez-Gallego <sup>a,b</sup>, Paula Bucci <sup>a,b</sup>, Raquel Lebrero <sup>a,b</sup> Raúl Muñoz <sup>a,b,\*</sup>

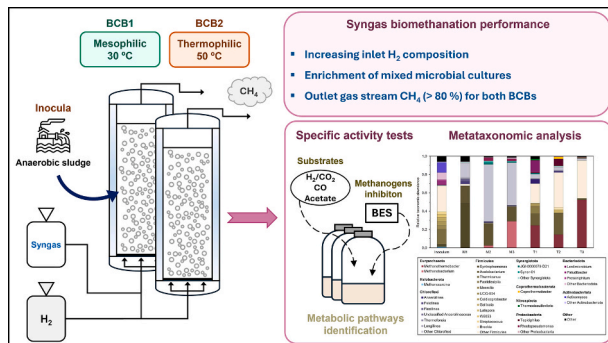
<sup>a</sup> Institute of Sustainable Processes, University of Valladolid, Paseo del Prado de la Magdalena 3-5, 47011 Valladolid, Spain

<sup>b</sup> Department of Chemical Engineering and Environmental Technology, University of Valladolid, Paseo del Prado de la Magdalena 3-5, 47011 Valladolid, Spain

## HIGHLIGHTS

- Mixed anaerobic broths were enriched into syngas biomethanation cultures.
- An output gas biomethane content of ~ 85 % was achieved in both bioreactors.
- Enrichment temperature shaped microbial diversity during biomethanation.
- Specific activity tests revealed the predominant metabolic pathways in the cultures.

## GRAPHICAL ABSTRACT



## ARTICLE INFO

**Keywords:**  
Biomethane  
Microbial enrichment  
Mixed microbial consortia  
Syngas biomethanation  
Temperature

## ABSTRACT

Syngas biomethanation—microbial conversion of CO<sub>2</sub>, CO, and H<sub>2</sub> into CH<sub>4</sub>—offers a promising strategy for upcycling gas streams from organic waste gasification. This study investigated the effect of temperature on microbial community enrichment and performance during syngas conversion in continuous bubble column bioreactors operated under mesophilic (30 °C) and thermophilic (50 °C) conditions at increasing H<sub>2</sub> loads. At the highest H<sub>2</sub> load, the CH<sub>4</sub> content in the biogas produced was approximately 84.6 ± 1.4 % under mesophilic conditions and 87.3 ± 1.3 % under thermophilic conditions. The study of the metabolic pathways revealed the dominance of syntrophic acetate oxidation, hydrogenotrophic methanogenesis, homoacetogenesis, and carboxydotrophic acetogenesis in the mesophilic consortium, while hydrogenotrophic methanogenesis and carboxydotrophic hydrogenogenesis dominated in the thermophilic consortium. Similarly, 16S rRNA metataxonomic analysis revealed shifts in microbial diversity, with *Methanobacterium*, *Acetobacterium*, and *Anaerolineaceae* dominating the mesophilic culture, and *Methanothermobacter* and carboxydotrophic *Firmicutes* accounting for almost the entire thermophilic community. These findings provide guidance for selecting mesophilic or thermophilic conditions based on preferred metabolic routes, microbial community composition, and process goals.

\* Corresponding author at: Institute of Sustainable Processes, University of Valladolid, Paseo del Prado de la Magdalena 3-5, 47011, Valladolid, Spain.  
E-mail address: [raul.munoz.torre@uva.es](mailto:raul.munoz.torre@uva.es) (R. Muñoz).

## 1. Introduction

The gradual replacement of fossil-derived energy sources has become essential from both environmental and economic perspectives, as global energy demand continues to rise (Mignogna et al., 2023). Biomethane is a renewable energy source primarily composed of pure methane ( $\text{CH}_4$ ), making it a flexible and valuable energy carrier in the industrial, transportation, building, and power & heat sectors (Calero et al., 2023). The EU dependence on natural gas imports reached 97 % in 2022 (European Biogas Association, 2023), highlighting the urgent need for measures to boost regional biomethane production. Biomethane can be produced either by biogas upgrading via removal of carbon dioxide ( $\text{CO}_2$ ) and trace components, or through gasification, followed by a methanation process (Meegoda et al., 2018). Gasification can overcome the limitations of anaerobic digestion via conversion of any type of waste, including recalcitrant organic waste, into a gas mixture (namely syngas) that can function as  $\text{CH}_4$  precursor.

Gasification comprises the partial oxidation of biomass or non-biodegradable organic waste products at high temperatures (between 600–900 °C) using a gasifying agent (i.e. air, oxygen) with the concomitant formation of a gas mixture composed of mainly carbon monoxide (CO), hydrogen ( $\text{H}_2$ ),  $\text{CO}_2$  and  $\text{CH}_4$  (Grimalt-Alemany et al., 2018; Latif et al., 2014; Westman et al., 2016). Syngas can be further converted into commercial products such as  $\text{CH}_4$ , fatty acids, carboxylic acids, alcohols and biopolymers (Asimakopoulos et al., 2018). Biological syngas methanation (biomethanation) has emerged as a promising alternative to catalytic methanation owing to its operation at ambient pressure and lower temperatures (30–55 °C), higher specificity for  $\text{CH}_4$ , and greater tolerance to inhibition by syngas pollutants (Henstra et al., 2007; Paniagua et al., 2022).

Syngas biomethanation can be carried out by mixed microbial consortia (MMC) (Asimakopoulos et al., 2020a; Rafrafi et al., 2021; Xu et al., 2020), obtained from sources such as anaerobic digestion sludges. This sludges represent a cheap and widely accessible MMC to function as inoculum for the start-up of syngas biomethanation systems (Laguillaumie et al., 2022). Syngas biomethanation by MMC stands as a highly robust and efficient metabolic process driven by the syntrophic interactions of a diverse group of anaerobic bacterial and archaeal species capable of converting CO and  $\text{H}_2/\text{CO}_2$  into  $\text{CH}_4$  (Asimakopoulos et al., 2020b).

The process is based on carboxydrophic hydrogenogenesis (water–gas shift reaction), carboxydrophic acetogenesis, hydrogenotrophic methanogenesis, acetoclastic methanogenesis, acetate oxidation (SAO) and homoacetogenesis (Asimakopoulos et al., 2020b; Grimalt-Alemany et al., 2018; Li et al., 2020). Carboxydrophic methanogenesis is another feasible reaction, although it does not play a significant role in CO conversion into  $\text{CH}_4$  in MMC (Grimalt-Alemany et al., 2020b; Kuipers and Kofoed, 2023).

Environmental factors such as pH and temperature play a fundamental role in syngas biomethanation. Most methanogenic archaea can grow within a pH range of 6.0 to 8.0, with optimal growth at pH 7.0, while bacteria present a broader pH range for optimal growth (Asimakopoulos et al., 2021b; Li et al., 2021). Temperature determines the occurrence of metabolic pathways and the kinetics of syngas biomethanation. Kinetic studies have reported that mesophilic conditions promote the development of carboxydrophic acetogenic species and the subsequent conversion to  $\text{CH}_4$  by acetoclastic methanogens. On the other hand, under thermophilic conditions, CO is converted almost exclusively to  $\text{H}_2$  and  $\text{CO}_2$  by carboxydrophic hydrogenogens and ultimately converted to  $\text{CH}_4$  via hydrogenotrophic methanogenic archaea (Grimalt-Alemany et al., 2020b; Hu et al., 2024).

Moreover, several studies have reported increased CO and  $\text{H}_2$  conversion rates and associated enhancement of  $\text{CH}_4$  productivity with rising operational temperature (Asimakopoulos et al., 2020b; Sieborg et al., 2025; Xu et al., 2020). However, thermophilic conditions also lead to reduced dissolved gas availability, which can limit biomethanation

performance, and increase operational costs compared to mesophilic conditions (Grimalt-Alemany et al., 2018). Consequently, exploring the effects of temperature and how it shapes microbial diversity is essential for tailoring bioreactor systems with optimized biomethanation performance.

An external addition of  $\text{H}_2$  to the syngas biomethanation bioreactor is typically required to reach a total conversion of  $\text{CO}_2$  and CO, and therefore high  $\text{CH}_4$  concentrations (Andreides et al., 2021). This  $\text{H}_2$  must be produced from water electrolysis powered via renewable electricity surplus to achieve a sustainable upgrading of syngas into biomethane (Asimakopoulos et al., 2021a).

To date, enrichment of anaerobic cultures for syngas biomethanation has been conducted in batch bottle systems (Arantes et al., 2018; García-Casado et al., 2024; Grimalt-Alemany et al., 2020b; Hu et al., 2024), while few studies have carried out methanogenic cultures enrichment in continuous bioreactors (Spyridonidis et al., 2023; Yun et al., 2017). These studies were focused on the enrichment of hydrogenotrophic cultures for biogas upgrading using CO-free syngas, without the addition of an external  $\text{H}_2$  supply. Direct enrichment of MMC in larger-scale, continuous bioreactors can facilitate the transfer of the system to industrial applications (Figueroa et al., 2021). This approach simplifies the scale-up process and may enhance microbial adaptation by reducing the time required for enrichment, as the larger supply of carbon and electron donors supports the proliferation of a significantly greater number of microbial generations (Luo and Angelidaki, 2013).

This work aimed at enriching and characterizing the performance of mesophilic and thermophilic MMC capable of performing syngas biomethanation at increasing loads of  $\text{H}_2$  in continuous lab-scale bubble column bioreactors (BCBs) with internal gas recirculation. To further characterize the culture enrichments, the microbial community structure was determined by means of 16S rRNA gene sequencing and the metabolic pathways involved in syngas biomethanation were elucidated via ad-hoc  $\text{H}_2/\text{CO}_2$ , CO, and acetate activity tests.

## 2. Materials and methods

### 2.1. Mineral salt medium and inoculum

The mineral salt medium used in all assays was a modified anaerobic basal medium (BA) (Asimakopoulos et al., 2020b; Jiang et al., 2023). Details regarding the composition and preparation of BA can be found in the *Supplementary Material*.

The inoculum for the syngas biomethanation reactors was prepared by mixing two different anaerobic sludges in a 1:1 vol ratio. The first sludge was collected from the mesophilic mixed anaerobic digester of Valladolid Wastewater Treatment Plant (Valladolid, Spain), and the second sludge from the thermophilic anaerobic digester of San Sebastian Urban Waste Treatment Plant (San Sebastian, Spain). The inoculum pH was  $8.28 \pm 0.05$  and contained  $77.77 \pm 0.93 \text{ g kg}^{-1}$  total solids (TS) and  $47.93 \pm 0.65 \text{ g kg}^{-1}$  volatile solids (VS).

### 2.2. Bubble column bioreactors configuration

Two identical transparent PVC BCBs (0.085 m internal diameter  $\times$  0.1 m height) with a working volume of 5 L were used for the enrichment of  $\text{H}_2$ -assisted syngas biomethanation microbial communities (*Supplementary Material*, Fig. S1). A handcrafted nitrile rubber membrane (0.5 mm pore size) was placed at the bottom of the bioreactors to allow gas sparging. Syngas (35:30:25:10 %v/v  $\text{H}_2:\text{CO}:\text{CO}_2:\text{CH}_4$ ) and  $\text{H}_2$  ( $\geq 99.9 \%$ ), purchased to Carburros Metálicos S.A. (Spain), were stored in 100 L gas-tight bags (MediSense, Netherlands) and injected in the bioreactors by means of peristaltic pumps (Watson Marlow, UK) and rotameters (Aalborg, USA) to control the gas inlet stream. The BCBs were also equipped with an internal gas recirculation operated at a ratio of 100 ( $Q_{\text{recirculation}}/Q_{\text{syngas}} = 100$ ) along the entire experimental period. BCB1 was operated at 30 °C (mesophilic conditions) and the

temperature of BCB2 was maintained at 50 °C (thermophilic conditions) in order to evaluate the influence of the temperature on the performance and microbial population structure of syngas-converting enrichments. These operational temperatures were selected to represent the lower boundaries of the mesophilic and thermophilic ranges, respectively, which are less frequently investigated in the literature compared to the more conventional 37 °C and 55 °C, and that will reduce operational costs. By employing 30 °C and 50 °C, the study aimed to characterize system behavior under suboptimal yet relevant operating conditions that may occur in practical applications where temperature control is limited or subject to fluctuations. Temperature was controlled with a water bath circulating system (Thermo Fisher Scientific, USA) interconnected to the external cylindrical jacket of the BCBs. The pH of the anaerobic culture broths was on-line measured and automatically adjusted to 7.0 ± 0.3 via a pH controller (EVOpHP5, BSV Electronic, Spain) with NaOH 2 M or HCl 2 M solutions.

### 2.3. Enrichment and process optimization

Three operational phases were set during the enrichment and optimization of syngas biomethanation communities in the BCBs under mesophilic and thermophilic conditions. Initially, each BCB was filled with 4.8 L of BA medium and flushed with syngas to ensure an anaerobic environment. Then, the BCBs were inoculated with 200 mL of sludge mix inoculum to reach a VS concentration of 0.96 ± 0.10 g L<sup>-1</sup>. The first experimental phase (Phase I) involved the acclimation of the mixed microbial community to the operational temperature and to syngas as the sole source of carbon and energy, which lasted for 42 days. The inlet syngas flowrate was set at 10 mL min<sup>-1</sup> (EBRT 500 min, syngas loading rate of 2.88 L<sub>syngas</sub> L<sup>-1</sup>reactor d<sup>-1</sup>) and maintained for all operational phases. Due to the incomplete stoichiometric conversion of CO and CO<sub>2</sub> into CH<sub>4</sub> during Phase I, pure H<sub>2</sub> was supplied from an additional gas-tight bag to the BCBs (Phase II) to modify the inlet gas composition (62.8:16.2:14.8:6.2 %v/v H<sub>2</sub>:CO:CO<sub>2</sub>:CH<sub>4</sub>). In addition, during Phase II (with a duration of 76 and 83 days for BCB1 and BCB2, respectively), a robustness test was performed to assess the influence of air intrusion on the consortium ability to recover its syngas biomethanation capacity. An air inlet stream of 1 L min<sup>-1</sup> was sparged overnight into the BCBs at day 90 (BCB1) and day 67 (BCB2). In Phase III, pure H<sub>2</sub> supply was increased to reach an inlet gas composition of 72.2:13.4:10.2:4.2 %v/v H<sub>2</sub>:CO:CO<sub>2</sub>:CH<sub>4</sub> in order to optimize syngas conversion into CH<sub>4</sub> for 37 and 93 days in BCB1 and BCB2, respectively.

Gas samples of 250 µL were taken periodically from the inlet and outlet of the BCBs to measure gas composition by GC-TCD. Liquid samples of 60 mL from the cultivation broth were harvested twice per week to determine the pH, concentration of dissolved total nitrogen (TN), dissolved organic carbon (TOC), volatile fatty acids (VFAs), TS and VS. In order to prevent nutrient limitation, 0.8 L of culture broth were withdrawn once per week in Phase I, centrifuged (4200 rpm, 20 min) and the biomass pellet was resuspended in fresh BA, flushed with syngas, and returned to the BCB. Due to the rapid depletion of nutrients in the culture during Phases II and III, the frequency of mineral medium replacement was increased to twice a week.

### 2.4. Activity tests

The elucidation of the metabolic pathways involved in the mesophilic and thermophilic syngas bioconversion into CH<sub>4</sub> in the BCBs was performed via activity tests conducted in 160 mL serum bottles. The assays employed syngas, CO, H<sub>2</sub>/CO<sub>2</sub>, or acetate as a carbon and energy source (Grimalt-Alemany et al., 2020b; Navarro et al., 2014). The initial conditions and substrates used in the tests are summarized in Table 1. Sodium 2-bromoethanesulfonate (BES) at a concentration of 15 mM was added to inhibit methanogenic archaea and quantify non-converted metabolites. All assays were carried out in triplicate.

The serum bottles were filled with 49 mL of BA medium and inoculated with 1 mL of cultivation broth from the corresponding BCB at the end of Phase III, previously centrifuged (10000 rpm, 5 min) and resuspended in 1 mL of fresh BA. BES or acetate were added, and the initial headspace composition was modified accordingly. The initial pH, pressure, headspace gas composition, biomass concentration (measured via optical density, OD), and VFAs were quantified. The average initial pH across all tests was 7.09 ± 0.04.

The syngas activity tests (Test series 1) were carried out in order to characterize possible intermediate products and evaluate the syngas-converting performance of all the microbial groups involved in the biomethanation process. Furthermore, the H<sub>2</sub>/CO<sub>2</sub> activity tests (Test series 2) in combination with the H<sub>2</sub>/CO<sub>2</sub> + BES activity tests (Test series 3) allowed for the identification of hydrogenotrophic methanogenic and homoacetogenic metabolic routes. Activity tests using CO (Test series 4) and CO + BES (Test series 5) were conducted to elucidate the presence of carboxydrophic acetogenic, hydrogenogenic and methanogenic catabolic routes in the enriched microbial cultures. Finally, the determination of the occurrence of acetoclastic pathways was accomplished via the acetate activity tests (Test series 6).

Test bottles were incubated in a rotary shaker at 250 rpm and the incubation temperature was set at 30 °C or 50 °C for tests inoculated with BCB1 and BCB2 cultures, respectively. The headspace composition, pressure, VFAs and biomass concentrations were monitored daily. The final pH of all tests was also recorded.

### 2.5. Calculations

The product yields in the activity tests were calculated as the number of moles of electrons integrated into the product *j* per number of moles of electrons released by the assimilation of substrates (electron yield) with equation 1 (Supplementary Material). Each mole of CO and H<sub>2</sub> dispenses two moles of electrons ( $n_{e^-H_2} = n_{e^-CO} = 2e^-mol$ ) (Asimakopoulos et al., 2020a).

The value of  $n_{e^-acetate}$  was 8 e<sup>-</sup> mol and  $n_{e^-(j)}$  was equal to 8 e<sup>-</sup> mol for CH<sub>4</sub> and 14 e<sup>-</sup> mol for propionate. Only acetate and propionate were considered in the metabolites yield calculation, as other VFAs were either not detected or were present at negligible concentrations during the activity tests.

Biomass yield in the activity tests was measured as volatile suspended solids (VSS) per mol of substrate and calculated with equation 2 (Supplementary Material).

The syngas quality index (SQI) represents the ratio of electron donors to carbon donors in syngas available for biomethanation and can be

**Table 1**

Initial conditions set in the activity tests performed with the mesophilic and thermophilic enriched microbial cultures.

Test series	Test condition	H <sub>2</sub> (atm)	CO <sub>2</sub> (atm)	CO (atm)	CH <sub>4</sub> (atm)	N <sub>2</sub> (atm)	Acetate (mM)	BES (mM)
1	Syngas	1	0.3	0.2	0.1	—	—	—
2	H <sub>2</sub> /CO <sub>2</sub>	1.2	0.4	—	—	—	—	—
3	H <sub>2</sub> /CO <sub>2</sub> + BES	1.2	0.4	—	—	—	—	15
4	CO	—	—	0.2	—	1.4	—	—
5	CO + BES	—	—	0.2	—	1.4	—	15
6	Acetate	—	—	—	—	1.6	25	—

calculated as described by Asimakopoulos et al. (2021a). An SQI of 4 indicates that, stoichiometrically, no compound would be limiting and that complete conversion of the substrates into  $\text{CH}_4$  is theoretically feasible. In contrast, an SQI below 4 indicates that carbon donors are in stoichiometric excess.

## 2.6. Analytical methods

The gaseous concentration of  $\text{CO}_2$ ,  $\text{CO}$ ,  $\text{CH}_4$ , and  $\text{H}_2$  were determined using a Bruker 430 gas chromatograph (Palo Alto, USA) equipped with a thermal conductivity detector and two capillary columns: CP-Molsieve 5 $\text{\AA}$  (15 m  $\times$  0.53 mm  $\times$  15  $\mu\text{m}$ ) and CP-PoraBOND Q (25 m  $\times$  0.53 mm  $\times$  10  $\mu\text{m}$ ). Oven, injector, and detector temperatures were maintained at 37, 150 and 200  $^{\circ}\text{C}$  for 5.5 min, respectively. Helium was employed as the carrier gas at 13.7  $\text{mL min}^{-1}$ .

The VFAs (acetate, propionate, butyrate, isobutyrate, valerate, iso-valerate) concentrations in the cultivation broth of the BCBs and activity test cultures were determined using 2 mL samples. The harvested culture was centrifuged at 10000 rpm for 10 min and the resulting supernatant was processed through a 0.22  $\mu\text{m}$  pore size filter. Finally, 1 mL of filtrate was acidified with 20  $\mu\text{L}$  of concentrated  $\text{H}_2\text{SO}_4$ . VFAs were then quantified in a gas chromatograph 7820A (Agilent, USA) equipped with a flame ionization detector, a G4513A autosampler and a Chromosorb W AW packed column (2 m  $\times$  1/8"  $\times$  2.1 mm SS) (10 % SP 1000, 1 %  $\text{H}_3\text{PO}_4$ , WAW 100/120). The injector, oven and detector temperatures were maintained at 375, 130 and 350  $^{\circ}\text{C}$ , respectively, while  $\text{N}_2$  was used as the carrier gas at 45  $\text{mL min}^{-1}$ .

The TS and VS concentrations in the inocula and BCBs cultivation broths were measured according to standard methods (Bridgewater et al., 2017). OD was measured at a wavelength of 600 nm using a spectrophotometer SPECTROstarNano (BMG LABTECH, Germany). A correlation between OD<sub>600</sub> and VSS concentration was established (Bridgewater et al., 2017). The pH was analyzed using a Basic 20 + pHmeter (Crison Instruments S.A., Barcelona). The TOC and TN concentrations of the BCB cultures were determined in a TOC-L<sub>CSH/CSN</sub> analyzer equipped with a TNM1 chemiluminescence unit (Shimadzu, Japan).

## 2.7. DNA extraction and microbial diversity analysis

Total genomic DNA was obtained from 2 mL samples collected from both the inocula and the culture aliquots from each of the BCBs under steady conditions in Phase I, II and III. Samples were stored at -20  $^{\circ}\text{C}$  until DNA extraction. Prior to the extraction, samples were centrifuged at 10000 rpm for 5 min and the resulting biomass was washed with 1X PBS. DNA was then isolated using the DNeasy PowerSoil Pro Kit (QIA-GEN, Germany). The final DNA concentration in the samples was quantified using a Qubit 4 Fluorometer (Thermo Fisher Scientific, USA).

Metataxonomic analysis was performed by Novogene (Cambridge, UK). 16S rRNA amplicon library generation and sequencing were performed in an Illumina NovaSeq 6000 instrument (paired-end 250 bp sequencing). PCR amplification of 16S rRNA gene V4 and V5 hyper-variable regions was carried out with 515F (5'-GTGCCAGCMGCCGCGGTAA-3') (Parada et al., 2016) and 907R primers (5'-CCGTCAATTCTTGTAGTTT-3') (Muyzer et al., 1995). Paired-end reads were assembled using FLASH V1.2.11 (Magoč and Salzberg, 2011). The bioinformatic pipeline to analyze Amplicon Sequencing data was completed with QIIME2 software (version QIIME2-202202). Denoising of de-duplicated sequences was performed with DADA2 method to generate Amplicon Sequence Variants (ASVs). Finally, ASVs were taxonomically annotated by means of rRNA database SILVA (version 138.1) (Quast et al., 2012) to discern microbial diversity in the samples. All the raw sequences data have been deposited in GenBank under BioProject PRJNA1221909. Principal Coordinate Analysis (PCoA) was performed in R (version 4.3.1) to visualize differences in microbial community composition across the collected samples, based on

weighted UniFrac distance metrics. The resulting PCoA plots were generated using the ggplot2 package (version 3.4.2).

## 3. Results and discussion

### 3.1. Performance of syngas biomethanation in bubble column bioreactors

The performance of the biomethanation process during culture enrichment was evaluated based on the  $\text{CH}_4$  content of the outlet biogas throughout the operational phases of the BCBs (Fig. 1). Additionally, the quantification of VFAs concentration provided further insights into the metabolism of the microbial consortia prevailing under the operational conditions of BCB1 and BCB2. The pH of the enrichment broths was maintained at 7.16  $\pm$  0.16 in BCB1 and 7.07  $\pm$  0.17 in BCB2 throughout the entire operation. The total dissolved nitrogen was also monitored to ensure that nutrient depletion did not limit  $\text{CH}_4$  production (Supplementary Material, Fig. S2).

The SQI of the inlet gas streams injected into the BCBs accounted for 1.18, 2.54 and 3.62 during the operational Phases I, II, and III, respectively. Therefore, a complete conversion of the electron donors ( $\text{H}_2$  and  $\text{CO}$ ) was theoretically achievable across all the experimental Phases.

The initial phase of the enrichment process involved the acclimation of the inoculum to syngas as the sole source of carbon and energy. A 2-day lag phase was observed before an increase in  $\text{CH}_4$  concentration in the outflow gas was detected under mesophilic and thermophilic conditions. During the start-up period, acetate rapidly accumulated in both bioreactors, with acetate concentrations in BCB1 (maximum of 2  $\text{g L}^{-1}$ ) ten times higher than those observed in BCB2. The endogenous degradation of the anaerobic sludge inoculum may have contributed to the VFAs production during the initial operation of the BCBs. Following this initial acclimation period, steady state was achieved, with  $\text{CH}_4$  concentrations reaching 37.3  $\pm$  1.3 % in BCB1 and 37.2  $\pm$  1.3 % in BCB2, while the contents of  $\text{CO}$  and  $\text{H}_2$  were approximately 1 % in the outlet gas streams of both BCBs. The low quality of the produced biomethane can be attributed to the composition of the supplied syngas, as indicated by its SQI, with  $\text{CO}_2$  content in the output gas under the steady state of 57.1  $\pm$  0.8 % and 56.3  $\pm$  0.6 % for BCB1 and BCB2, respectively.

The additional  $\text{H}_2$  supplied to the bioreactors during Phase II increased the  $\text{CH}_4$  content in the upgraded gas up to 71.1  $\pm$  0.4 % in BCB1 by day 104, as anticipated with the higher SQI of 2.54. Similarly, the  $\text{CH}_4$  concentration in the upgraded gas in BCB2 increased up to 66.4  $\pm$  2.6 % by day 60 (prior to the robustness test). However, after the tests, the  $\text{CH}_4$  concentration in the upgraded gas stabilized at a lower and more variable steady state concentration of 56.5  $\pm$  2.1 %  $\text{CH}_4$ . After the robustness test,  $\text{CO}$  conversion remained high, supporting  $\text{CO}$  concentrations below 2 % in the upgraded gas in both BCBs. Nonetheless,  $\text{H}_2$  was not fully converted.  $\text{H}_2$  supplementation in Phase II induced a rapid VFAs accumulation in BCB1, mainly acetate, which reached concentrations above 7.1  $\text{g L}^{-1}$ . Similarly, acetate and propionate were the main VFAs accumulated in BCB2 in Phase II, but their concentration did not reach values over 0.2  $\text{g L}^{-1}$ . A sudden increase in  $\text{H}_2$  partial pressure can foster the development of homoacetogens in MMC, suggesting that the additional  $\text{H}_2$  supplied to BCB1 may have shifted the syngas conversion routes, favoring acetate production (Rafrafi et al., 2021; Tsapekos et al., 2022). Therefore, the accumulation of acetate and  $\text{H}_2$  depletion likely facilitated SAO metabolism, which contributed to the observed consumption of VFAs in the cultivation broth by the end of Phase II.

The impact of air intrusion on the ability of the consortium to maintain the biomethanation performance was evaluated during Phase II in each of the BCBs during the robustness test. The combined effects of starvation and  $\text{O}_2$  exposure resulted in a reduction in  $\text{CH}_4$  levels in the upgraded gas in both bioreactors. Nevertheless, the biomethanation performance in BCB1 exhibited a rapid recovery in the subsequent days, with  $\text{CH}_4$  contents of 59.8  $\pm$  1.1 % after 8 h from the interruption of air supply. Steady state  $\text{CH}_4$  contents of 66.3  $\pm$  2.4 % were recorded at the end of Phase II. Interestingly, the accumulated VFAs in BCB1 were

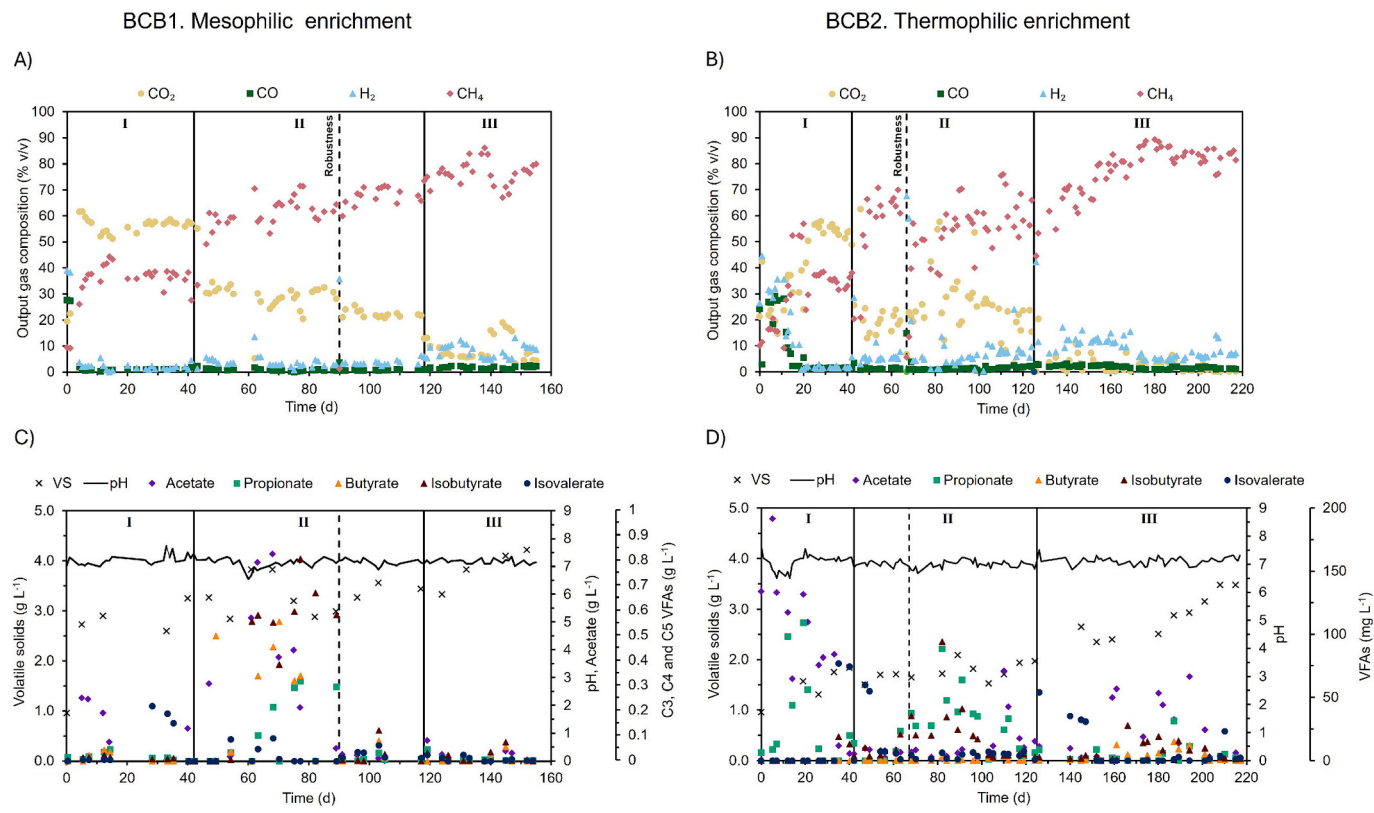


**Fig. 1.** Time course of the outflow gas composition in A) BCB1 and B) BCB2, and of volatile solids (VS), pH, acetate, propionate, butyrate, isobutyrate and isovalerate in C) BCB1 and D) BCB2. Operational phases are delimited with a vertical continuous line. The dashed line represents the robustness test performed in each reactor.

rapidly degraded during air exposure, likely due to the presence of facultative anaerobic microorganisms, which suggests that the absence of syngas electron donors restricted VFAs production. In contrast, the biomethanation capacity of the microbial community present in BCB2 was more severely affected by the presence of O<sub>2</sub> compared to that in BCB1. Indeed, 16 days were needed to reach CH<sub>4</sub> levels over 50 %, and steady state CH<sub>4</sub> contents of 56.5 ± 2.1 % were recorded in the upgraded gas from day 71 onwards. Indeed, oxygen can severely impact syngas biomethanation, as methanogenic archaea are highly susceptible to inhibition under aerobic environments. However, studies have indicated that methanogens can remain viable even after several hours of air exposure (Jarrell, 1985). Additionally, MMC typically exhibit a greater tolerance to air than isolated strains, due to the inherent presence of facultative anaerobes capable of in-situ depleting the dissolved O<sub>2</sub> in the cultivation broth (Kato et al., 1993). These findings confirmed that the MMC developed in the BCBs exhibit robust biomethanation capabilities and may be effectively utilized in biological methanation systems without the risk of irreversible process collapse due to incidental O<sub>2</sub> intrusions.

During operational Phase III, both BCBs achieved the maximum CH<sub>4</sub> content in the upgraded gas, which was aligned with the higher SQI of the inlet gas. Steady state CH<sub>4</sub> contents of 84.6 ± 1.4 % and 87.3 ± 1.3 % were recorded in Phase III in BCB1 and BCB2, respectively. This finding is consistent with observations from a batch thermophilic biomethanation system operated at 50 °C, where methanogenesis is enhanced under high H<sub>2</sub> partial pressure (Palacios et al., 2025). Contrary to the expected, H<sub>2</sub> was not fully converted during Phase III. However, the carbon donors (CO and CO<sub>2</sub>) remained below 1 % in the upgraded gas during steady state conditions. In this context, a 0.18 L biomethanation trickle-bed reactor supplied with syngas (SQI = 3.67, EBRT = 3h) exhibited a CH<sub>4</sub> composition of 71.7 % in the upgraded gas when operated under mesophilic conditions (37 °C) and 71.2 % under thermophilic (60 °C) conditions. However, the H<sub>2</sub> conversion rate was

found to be nearly 100 % under both operational conditions (Asimakopoulos et al., 2021a). Although similar thermophilic BCB systems have reported H<sub>2</sub>/CO<sub>2</sub> conversion rates as high as 94 % (Laguillaumie et al., 2022), the incomplete H<sub>2</sub> utilization observed in our system suggests that gas mass transfer limitations may have constrained the efficiency of biomethanation. Another study reported that slightly reducing the H<sub>2</sub> flow supply by 7.5 % relative to stoichiometry requirements improved H<sub>2</sub> conversion rates in a trickle-bed biomethanation reactor (Sposób, 2024). The operational parameters, reactor scale, and microbial dynamics likely contributed to the higher H<sub>2</sub> conversion in the referenced trickle-bed reactor, thus further investigation into these factors is needed to optimize microbial efficiency and minimize H<sub>2</sub> losses in the BCBs.

Since the concentration of VFAs remained below inhibitory values, sufficient electron acceptors were supplied, and the pH was controlled at optimum values for biomethanation. The presence of H<sub>2</sub> in the upgraded gas during Phases II (3.3 ± 0.5 % H<sub>2</sub>) and III (5.6 ± 0.6 % H<sub>2</sub>) in both BCBs suggested that mass transfer limitations hindered the availability of H<sub>2</sub> for the microorganisms. Despite the high CH<sub>4</sub> content achieved in the upgraded syngas during the final experimental phase in both BCB1 and BCB2, a higher biomethane purity is required for its direct injection into the natural gas grid. Therefore, a further optimization of operational parameters such as the SQI, gas residence time and internal gas recirculation rate may improve CH<sub>4</sub> yields and H<sub>2</sub> conversion rates, thereby contributing to the optimization of the biomethanation process in the BCBs (Gavala and Skidas, 2025).

Acetate was the predominant accumulated metabolite in the cultivation broth during Phase III in BCB1, reaching concentrations of approximately 0.7 g L<sup>-1</sup>. Interestingly, these levels were substantially lower than the VFAs accumulation observed during Phases I and II. However, VFA concentrations were close to zero by the end of the enrichment process. A similar accumulation of VFAs occurred during Phase III in BCB2, although the concentrations of these organic

compounds remained below 75 mg L<sup>-1</sup>. This finding suggests the presence of microorganisms from the acetoclastic trophic group, which may scavenge VFAs from the BCB1 culture (García-Casado et al., 2024; Grimalt-Alemany et al., 2020b). Biomass concentration in both BCB1 and BCB2 reached maximum values during Phase III. The steady state biomass content in BCB1 (4.2 ± 0.1 g VS L<sup>-1</sup>) was higher than that observed in BCB2 (3.4 ± 0.2 g VS L<sup>-1</sup>), which was consistent with the higher biomass yield calculated for the mesophilic enriched consortium in the syngas activity test, compared to the thermophilic consortium.

### 3.2. Identification of syngas biomethanation pathways

The results of the specific activity tests, which were conducted to analyze the metabolism of the mesophilic and thermophilic microbial communities enriched in BCB1 and BCB2, respectively, are presented in Table 2. The syngas specific activity tests were carried out to evaluate the overall performance of the mesophilic and thermophilic enriched consortia. Differences were observed in the profiles obtained for the gas conversion and products generated between consortia (Supplementary Material, Fig. S3). The conversion of syngas by the mesophilic enriched consortium resulted in CH<sub>4</sub> (Supplementary Material, Fig. S3A) and acetate in the initial stages of the experiments (Supplementary Material, Fig. S3C). Acetate reached a maximum concentration of 7.77 ± 0.48 mM and was further converted into CH<sub>4</sub> (0.44 ± 0.04 e-mol yield). In contrast, the thermophilic enriched community performed syngas biomethanation (0.70 ± 0.01 e-mol CH<sub>4</sub> e-mol<sup>-1</sup> substrates) (Supplementary Material, Fig. S3B) with a residual acetate accumulation (0.01 ± 0.00 e-mol acetate e-mol<sup>-1</sup> substrates) (Supplementary Material, Fig. S3D). These empirical findings suggest that temperature led to enrichments that convert syngas into CH<sub>4</sub> through different metabolic pathways.

On the other hand, the mesophilic enriched culture under an initial H<sub>2</sub>/CO<sub>2</sub> atmosphere initially synthesized CH<sub>4</sub> (Supplementary Material, Fig. S4A) while acetate rapidly accumulated until gaseous substrates depletion (Supplementary Material, Fig. S4C). Subsequently, acetate was degraded to produce CH<sub>4</sub>, resulting within an e-mol yield of 0.90 ± 0.01. Tests supplied with H<sub>2</sub>/CO<sub>2</sub> and BES resulted in the depletion of

gaseous substrates (Supplementary Material, Fig. S4E) and the subsequent accumulation of acetate as the main end-product (0.72 ± 0.02 e-mol acetate e-mol<sup>-1</sup> substrates) and minor propionate concentrations (0.020 ± 0.001 e-mol propionate e-mol<sup>-1</sup> substrates) (Supplementary Material, Fig. S4G). Thus, homoacetogenesis and hydrogenotrophic methanogenesis acted as competing H<sub>2</sub>-depleting catabolic routes in the mesophilic anaerobic MMC, which is supported by multiple studies (Asimakopoulos et al., 2020b; Grimalt-Alemany et al., 2020b; Liu et al., 2016). Notably, it was observed that acetate was eventually converted into CH<sub>4</sub>, highlighting the role of VFAs as intermediate metabolites in mesophilic syngas biomethanation. On the contrary, H<sub>2</sub>/CO<sub>2</sub> conversion by the thermophilic enriched consortium resulted in the production of CH<sub>4</sub> as the primary end-product (0.79 ± 0.01 e-mol yield) (Supplementary Material, Fig. S4B). Indeed, a negligible concentration of acetate was accumulated at the end of the thermophilic tests, yielding 0.01 ± 0.00 e-mol acetate per e-mol of H<sub>2</sub> (Supplementary Material, Fig. S4D). The fact that the activity tests with H<sub>2</sub>/CO<sub>2</sub> BES (Supplementary Material, Fig. S4F and S4H) did not exhibit metabolic activity suggests that hydrogenotrophic methanogenesis was the key catabolic route responsible for CH<sub>4</sub> production from H<sub>2</sub>/CO<sub>2</sub> in the thermophilic enriched consortium from BCB2, while homoacetogenesis could have been present to a lesser extent.

During the CO activity tests, the mesophilic enriched community rapidly converted CO into acetate (Supplementary Material, Fig. S5C), which was then converted into CH<sub>4</sub>, achieving an e-mol yield of 0.75 ± 0.03 e-mol CH<sub>4</sub> e-mol<sup>-1</sup> CO (Supplementary Material, Fig. S5A). Inhibition of mesophilic methanogens with BES resulted in the accumulation of acetate (0.55 ± 0.01 e-mol yield), with no apparent depletion of the metabolites produced from CO (Supplementary Material, Fig. S5E and S5G). Additionally, a similar acetate e-mol recovery was observed in CO activity batch tests reported in literature. Sancho Navarro et al. (2016) have reported that CO (initial p<sub>CO</sub> = 0.2 atm) was converted by mesophilic MMC inhabiting anaerobic sludge primarily via carboxydrophic acetogenesis (0.51 ± 0.08 e-mol acetate e-mol<sup>-1</sup> CO) when BES (50 mM) was added to the cultures. This finding, along with the data extracted from the herein conducted metabolic assays, implies that carboxydrophic acetogenesis may be the predominant CO-consuming

**Table 2**  
Final pH, biomass yield and product recovery in the activity tests conducted with the mesophilic and thermophilic enriched microbial communities.

Activity test	Final pH	Biomass yield (g VSS mol <sup>-1</sup> )	Product yield (e-mol product (e-mol substrates) <sup>-1</sup> )				Product recovery (% e-mol products (e-mol substrates) <sup>-1</sup> )
			CH <sub>4</sub>	Acetate	Propionate	H <sub>2</sub>	
<b>Mesophilic enriched microbial community</b>							
Syngas	7.18 ± 0.06	1.06 ± 0.01	0.44 ± 0.04	—	—	—	43.68 ± 4.56
H <sub>2</sub> /CO <sub>2</sub>	7.54 ± 0.05	0.36 ± 0.03	0.90 ± 0.01	—	—	—	90.84 ± 1.48
H <sub>2</sub> /CO <sub>2</sub> + BES	7.31 ± 0.07	0.75 ± 0.03	—	0.72 ± 0.02	0.020 ± 0.001	—	73.94 ± 2.22
CO	7.49 ± 0.08	2.22 ± 0.24	0.75 ± 0.03	—	—	—	76.37 ± 4.36
CO + BES	7.17 ± 0.02	2.27 ± 0.15	—	0.55 ± 0.01	0.001 ± 0.000	—	55.18 ± 0.99
Acetate	7.54 ± 0.12	0.32 ± 0.06	0.70 ± 0.03	—	—	—	69.64 ± 3.16
<b>Thermophilic enriched microbial community</b>							
Syngas	7.67 ± 0.08	0.67 ± 0.02	0.70 ± 0.01	0.01 ± 0.00	—	—	71.72 ± 1.06
H <sub>2</sub> /CO <sub>2</sub>	7.60 ± 0.05	0.65 ± 0.02	0.79 ± 0.01	0.01 ± 0.00	—	—	79.66 ± 0.71
H <sub>2</sub> /CO <sub>2</sub> + BES	7.09 ± 0.04	—	—	—	—	—	—
CO	7.73 ± 0.05	0.88 ± 0.02	0.65 ± 0.01	0.07 ± 0.01	—	—	71.35 ± 2.42
CO + BES	7.60 ± 0.02	0.20 ± 0.03	—	0.09 ± 0.02	—	0.74 ± 0.02	98.48 ± 7.02
Acetate	7.11 ± 0.03	—	—	—	—	—	—

metabolic pathway involved in syngas biomethanation carried out by the mesophilic enriched consortium.

On the other hand, the tests with the thermophilic enriched culture demonstrated that CO was consumed with a simultaneous  $\text{CH}_4$  release ( $0.65 \pm 0.01$  e-mol yield) (Supplementary Material, Fig. S5B). Acetate was also produced from CO, although the yield was low ( $0.07 \pm 0.01$  e-mol of acetate produced for e-mol of CO) (Supplementary Material, Fig. S5D). Additionally, no further conversion of the metabolites occurred. Upon addition of BES, CO continued to be consumed by the thermophilic microbial consortium, but no  $\text{CH}_4$  was produced (Supplementary Material, Fig. S5F). Instead, equal concentrations of  $\text{H}_2$  and  $\text{CO}_2$  and a minor acetate accumulation (Supplementary Material, Fig. S5H) were detected. The distinct metabolite production profile observed in specific tests with CO, without BES addition and with methanogenesis inhibition, suggest that the thermophilic enriched consortium was able to convert CO indirectly into  $\text{CH}_4$ , with  $\text{H}_2$  acting as intermediate metabolite. This pattern was consistent with findings from similar CO activity tests utilizing thermophilic syngas-consuming MMC (Grimalt-Alemany et al., 2020b). It can be hypothesized that carboxydrotrophic hydrogenogenesis was the dominant CO-converting metabolic route within the thermophilic microbial consortium (Hu et al., 2024), although carboxydrotrophic acetogenesis may also occur at low rates and carboxydrotrophic methanogenesis remains feasible.

The specific acetate consumption experiments revealed that the mesophilic enriched community degraded acetate while  $\text{CH}_4$  was simultaneously produced as the main end-metabolite, yielding  $0.70 \pm 0.03$  e-mol  $\text{CH}_4$  e-mol $^{-1}$  acetate (Supplementary Material, Fig. S6A and S6C). Conversely, the thermophilic microbial consortium exhibited no activity when acetate was used as the sole source of carbon and energy (Supplementary Material, Fig. S6B and S6D). In this context, acetoclastic methanogenesis typically governs acetate conversion in mesophilic microbial consortia-driven syngas biomethanation due to its thermodynamically favorable reaction compared to SAO ( $\Delta G^\circ = -31$  kJ mol $^{-1}$  and  $\Delta G^\circ = +104.6$  kJ mol $^{-1}$  for acetoclastic methanogenesis and SAO, respectively) (Grimalt-Alemany et al., 2018). However, coupling acetate oxidation with the hydrogenotrophic methanogenesis pathway overcomes the energetic limitations, making acetate degradation via SAO feasible ( $\Delta G^\circ = -31$  kJ mol $^{-1}$  for the combined reaction) (Hattori, 2008). Moreover, kinetic models of syngas conversion by mesophilic MMC have demonstrated that high acetate concentrations and low  $\text{H}_2$  partial pressure enabled SAO to play a significant role in acetate degradation through this metabolic pathway, under the reported operating conditions (Grimalt-Alemany et al., 2020a).  $\text{H}_2$  in the headspace may not have been detectable due to the rapid consumption of the produced gas by hydrogenotrophic methanogens or the presence of other syntrophic relationship mechanisms, such as direct interspecies electron transfer.

Additionally, high acetate concentrations are known to be inhibitory to acetoclastic methanogens as a result of their limited tolerance to acetate accumulation (Pan et al., 2021). Thus, considering that no species from the acetoclastic methanogenic trophic group were identified at significant levels during any of the enrichment phases in BCB1, acetate and VFAs likely acted as intermediates preferentially depleted via the SAO pathway rather than through direct acetoclastic methanogenesis. On the other hand, the absence of acetate consumption during the experiments incubated at 50 °C suggests that both acetoclastic methanogenesis and SAO may not have been significantly relevant metabolic pathways for biomethanation by the thermophilic community enriched in BCB2 by the end of Phase III.

Overall, the calculated e-mol recovery of the quantified products showed a good consistency and values over 70 %, except in the mesophilic tests conducted with syngas and CO in the presence of BES. Other compounds (e.g. bioalcohols, biopolymers) have been identified in syngas-fermenting MMC systems in literature (Asimakopoulos et al., 2018). Some species of *Acetobacterium* have been shown to produce ethanol via the carboxydrotrophic metabolic route (Arantes et al., 2020),

and *Rhodopseudomonas* has been shown to be able to accumulate poly-hydroxyalkanoates from VFAs (acetate and propionate) (Wu et al., 2012). This could indicate that unquantified byproducts may have accumulated in the culture during syngas conversion by the enriched mesophilic consortium, thereby interfering with the estimated product recovery. Additionally, the test inoculated with the mesophilic enriched community and supplied with CO and BES exhibited the highest biomass yield ( $2.27 \pm 0.15$  g VSS mol $^{-1}$ ). Mesophilic acetogenic carboxydrotrophs have been shown to be more energy-efficient than other syngas-converting microorganisms in MMC. Similar biomass yields ( $2.45 \pm 0.06$  g VSS mol $^{-1}$ ) were reported for this microbial trophic group in methanogen-inhibited specific activity tests conducted by Grimalt-Alemany et al. (2020b) and inoculated with a mesophilic syngas-converting enriched MMC under a CO atmosphere ( $p_{\text{CO}} = 0.4$  atm) as the sole carbon source, which was consistent with the lower product recovery recorded in our batch assays.

### 3.3. Microbial community analysis

The bacterial and archaeal community were analyzed in the initial inoculum and at the end of each operational phase (I, II, III) in BCB1 and BCB2 to assess the impact of the enrichment process on microbial diversity. A total of 1304 ASVs were obtained, indicating that several microbial species were involved in the enrichment. The initial inoculum comprised the most diverse microbial community (Simpson index of 0.970), whereas all BCBs samples exhibited more uniform microbial communities (Simpson indices of 0.736 for BCB1 and 0.669 for BCB2, at phase III) (Supplementary material, Table S1). These findings suggest that mesophilic and thermophilic biomethanation enrichment processes resulted in a less complex microbial community, which was also observed in other syngas-utilizing enrichment studies as a result of the limited carbon spectrum of syngas (Grimalt-Alemany et al., 2020b; Liu et al., 2018).

The relative abundances of the main phyla and genera identified are represented in Fig. 2. Most of the microbial genera detected in the inoculum were not discerned in any of the BCBs samples or showed minor relative abundance (except for *Caldicoprobacter* and *Syntrophomonas*). Moreover, microbial diversity largely diverged in BCB1 and BCB2, which suggests that temperature promoted a strong shift in the microbial community during the culture enrichment. This behavior is also reflected in the PCoA (Fig. 3), where two different groups were clearly separated. Additionally, the inoculum clustered apart from both groups. One cluster comprised BCB1 samples, while the other included BCB2 samples, supporting that each temperature condition shaped the microbial community in a significantly distinct manner and led to the enrichment of specific microbial groups. The thermophilic enrichment samples showed a more concentrated distribution, indicating lower community variability across the different operational Phases of BCB2 compared to BCB1.

The composition and relative abundance of the microbial consortia in BCB1 during the enrichment exhibited differences in each operational phase. The main phyla characterized in BCB1 samples were *Euryarchaeota*, *Firmicutes*, *Chloroflexi*, *Proteobacteria* and *Synergistota*. The only archaeal genus detected in BCB1 with significant abundance was *Methanobacterium*. Indeed, its relative abundance increased from < 0.1 % (M1) and 2.4 % (M2) to 28.9 % in the final enriched microbial culture (M3). The *Firmicutes* phylum in M1 was dominant (69.6 %), but its relative abundance decreased in M2 (24.7 %) and M3 (16.3 %). *Syntrophomonas* and *Acetobacterium* represented more than 98 % of the *Firmicutes* phylum in BCB1 samples. Despite *Syntrophomonas* being the most abundant genus at the end of the first Phase of BCB1 enrichment (M1, 48.6 %), its presence was negligible in M2 and M3 (< 0.01 %). Nevertheless, the genus *Acetobacterium* consistently maintained a significant presence throughout all three enrichment phases (19–24 %). In addition, the phylum *Chloroflexi* led the microbial community diversity developed in BCB1, particularly in Phases II and III where it reached

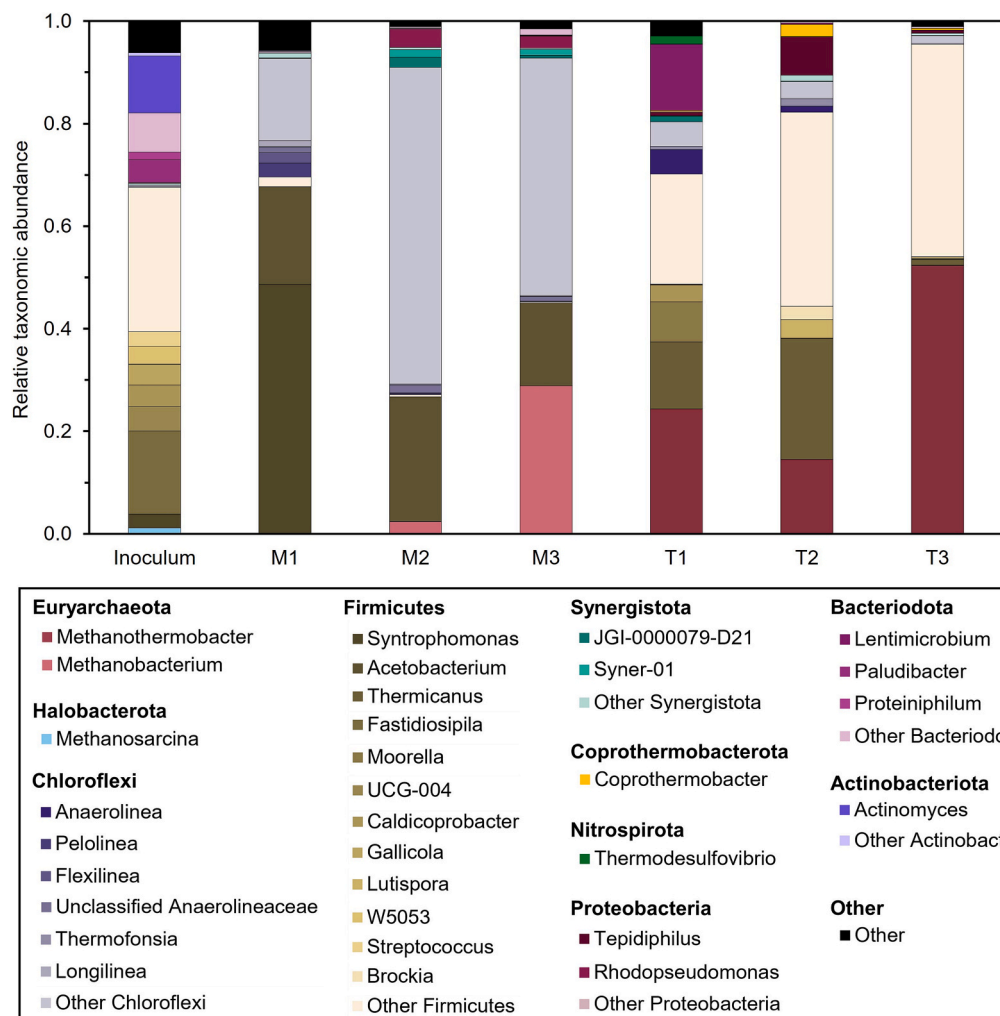


**Fig. 2.** Relative taxonomic abundance of annotated ASVs of the initial inoculum and BCBs microbial consortia. M1, M2 and M3 refer to samples withdrawn from BCB1 at the end of Phase I, II and III, respectively. T1, T2 and T3 refer to samples withdrawn from BCB2 at the end of Phase I, II and III, respectively.

shares of 63.8 % and 47.6 %, respectively. Interestingly, more than 95 % of the ASVs classified under *Chloroflexi* phylum belonged to the *Anaerolineaceae* family. *Synergistota* and *Proteobacteria* were also observed as part of the microbial consortium in all BCB1 Phases (0.9–3.9 %).

The metabolism of *Methanobacterium* supports the production of CH<sub>4</sub> from H<sub>2</sub>/CO<sub>2</sub> or formate (Holmes and Smith, 2016). This genus has been typically identified in mesophilic mixed microbial communities from bioreactors supplied with syngas (Cheng et al., 2022; Jiang et al., 2023; Sposób, 2024; Thapa et al., 2022). Mesophilic temperatures have been shown to promote the enrichment of the *Methanobacterium* archaeal population in H<sub>2</sub>/CO<sub>2</sub>-converting systems (Rafrafi et al., 2021). The increasing availability of H<sub>2</sub> during operational Phases II and III supported the development of the *Methanobacterium* genus. The genus *Syntrophomonas* has been reported to degrade VFAs, exclusively when hydrogenotrophic microorganisms are present (Sousa et al., 2007). The low concentration of VFAs observed at the end of Phase I under mesophilic conditions could have supported the high abundance of *Syntrophomonas* in the microbial consortium. The *Acetobacterium* genus is known to consist of anaerobic homoacetogenic bacteria, with several species also associated with carboxydrophic acetogenic growth (Ross et al., 2020). Members of the *Acetobacterium* genus have been frequently observed in enriched syngas-converting mesophilic consortia (Arantes et al., 2018; Cheng et al., 2022; García-Casado et al., 2024; Grimalt-Alemany et al., 2020b; Sancho Navarro et al., 2016; Tunca et al., 2025). Consequently, *Acetobacterium* species were likely responsible for

the production of VFAs from both H<sub>2</sub>/CO<sub>2</sub> and CO in BCB1. *Acetobacterium* might have outcompeted the methanogenic archaea in Phase I of the BCB1 enrichment, which could explain the low abundance of *Methanobacterium* in M1. The *Anaerolineaceae* bacteria are chemoheterotrophic microorganisms found in methanogenic sludge reactors associated to cell debris and dissolved organic matter recycling (Bovio-Winkler et al., 2023). Both *Anaerolineaceae* (Zeng et al., 2024) and *Synergistota* (Chen et al., 2024) can establish a syntrophic association with hydrogenotrophic methanogens, which supports the active CH<sub>4</sub> production observed in BCB1.

Similarly, the diversity of the microbial consortium underwent significant variations over the course of the thermophilic enrichment. Overall, the microbial consortia enriched in BCB2 was composed of *Euryarchaeota*, *Firmicutes*, *Chloroflexi*, *Bacteroidota*, *Proteobacteria*, *Synergistota*, *Coprothermobacterota* and *Nitrospirota*. *Methanothermobacter* was the only genus detected from the *Euryarchaeota* phylum, with a relative abundance ranging from 14–24 % in T1 and T2, and reaching 52.4 % by the end of the enrichment (T3). *Firmicutes* was one of the dominant phyla developed in BCB2, comprising between 43 and 67 % of the microbial community across all operational phases. The main genera classified within *Firmicutes* were *Moorella* (7.9 %) and *Caldicoprobacter* (3.3 %) in T1, *Lutispora* (3.6 %) and *Brockia* (2.5 %) in T2, while *Thermicanus* (13–26 %) was observed in both T1 and T2. *Chloroflexi* was not as dominant in BCB2 microbial consortia compared to BCB1, and it was even less abundant in T3 (from 10.2 % in T1 to 1.7 % in T3). *Bacteroidota*

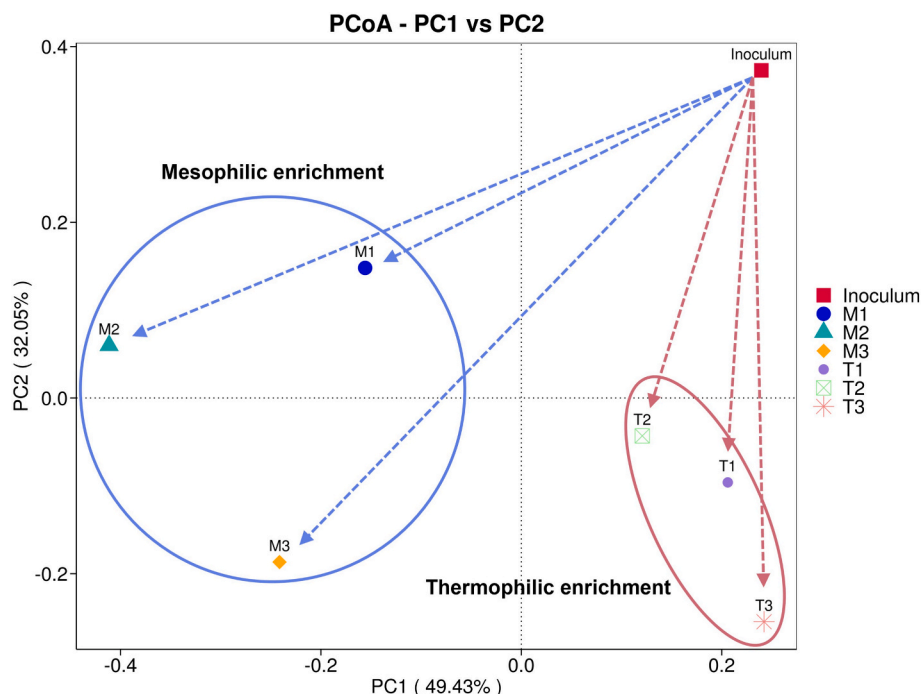


**Fig. 3.** Principal Coordinates Analysis (PCoA) based on Weighted UniFrac distance of mesophilic and thermophilic enriched microbial communities. M1, M2 and M3 refers to samples withdrawn from the BCB1 at the end of Phase I, II and III, respectively. T1, T2 and T3 refers to samples withdrawn from the BCB2 at the end of Phase I, II and III, respectively.

(13.0 %) and *Nitrospirota* (1.6 %) were only present at significant levels in T1, while *Proteobacteria* (7.6 %) and *Coprothermobacterota* (2.4 %) were relevant in T2. *Synergistota* represented less than 0.4 % of the total microbial community present at the end of Phase III (1.2 % in T1 and T2).

*Methanothermobacter* archaea are hydrogenotrophic methanogens adapted to thermophilic and extremely thermophilic environments (Laguillaumie et al., 2022). This genus is considered a key group of methanogens in systems devoted to syngas or  $H_2/CO_2$  conversion under thermophilic conditions (Asimakopoulos et al., 2020b; Biderre-Petit et al., 2024; Goonesekera et al., 2024; Grimalt-Alemany et al., 2020b; Keramati et al., 2024; Laguillaumie et al., 2022; Li et al., 2021, 2022; Zheng et al., 2023). The long-term operation of BCB2 under thermophilic conditions, coupled with the high  $H_2$  content in the gas injected during T3, likely facilitated the dominance of *Methanothermobacter* in the microbial community, as observed by Zheng et al. (2023). Additionally, *M. thermautrophicus* has been demonstrated to utilize CO as its sole energy source (Omae et al., 2019), suggesting that *Methanothermobacter* species may have potentially used inlet CO for growth during BCB2 operation. However, the activity tests herein indicated that carboxydrophic hydrogenogens were involved in CO metabolism, at least during the final phase of the enrichment. The phylum *Firmicutes*, known to contain the majority of identified carboxydrophic bacteria, has been associated with  $H_2/CO_2$  production from CO in a trickling-bed reactor devoted to syngas biomethanation (Goonesekera et al., 2024). Therefore, unclassified *Firmicutes* strains in BCB2 may have carried out carboxydrophic hydrogenogenesis.

Another genus detected in BCB2 that is capable of consuming CO was *Moorella* (Zheng et al., 2023). *Moorella* consists of homoacetogenic bacteria that can also produce acetate from CO as the primary end product, making syngas fermentation a suitable process for these bacteria. Then, the accumulation of acetate in the initial stages of T1 could be associated to the presence of *Moorella* in BCB2. The genus *Lutispora* has been identified as part of the mixed microbial communities involved in synthetic gas conversion in our particular study (Asimakopoulos et al., 2020b; Grimalt-Alemany et al., 2020b). *Lutispora* has been

associated with the production of VFAs (acetate, propionate, isobutyrate and isovalerate) from amino acids (Keramati et al., 2024). Hence, *Lutispora* may have contributed to cellular debris recycling and VFAs production during T2.

Other thermophilic bacteria identified in T1 and T2 harbor the SAO metabolism, including *Synergistota*, *Anaerolinea* (*Chloroflexi*), *Caldicoprobacter* (*Firmicutes*) (Dyksma et al., 2020), *Coprothermobacter* (*Coprothermobacterota*) (Morgan-Sagastume et al., 2019), *Tepidiphilus* (*Proteobacteria*) (Keramati et al., 2024), and *Lentimicrobium* (*Bacteroidota*) (Zheng et al., 2019). These genera have thus been potentially linked to the degradation and production of short-chain VFAs, based on the partial pressure of gases. Metabolic interactions between the diverse identified syntrophic bacteria and the methanogenic archaea *Methanothermobacter* may have dominated syngas conversion in T1 and T2 samples of BCB2, following a similar commensalism observed in BCB1.

Overall, considering the results from the activity tests and the analysis of the structure of the microbial consortia in BCB1, the proposed metabolic network for syngas biomethanation carried out by the mesophilic enriched consortium suggests that the  $H_2/CO_2$  present in syngas could have been converted directly into  $CH_4$  via the hydrogenotrophic methanogenic pathway (mediated by *Methanobacterium*) and into VFAs (mainly acetate) via the homoacetogenic pathway (carried out by *Acetobacterium*). Additionally, the CO present in syngas may have been primarily converted into VFAs through the carboxydrophic metabolism of *Acetobacterium*. Furthermore, the SAO bacteria identified in BCB1 may have also degraded VFAs into  $H_2/CO_2$  or formate, which were then utilized by *Methanobacterium* for  $CH_4$  production. Direct interspecies electron transfer may also explain the commensal relationship between SAO bacteria and methanogens in the generation of  $CH_4$  from VFAs within the BCB1 enriched consortium. On the contrary, the enriched microbial consortium developed in BCB2 achieved syngas biomethanation mainly via the direct hydrogenotrophic pathway (with *Methanothermobacter*) and the indirect conversion of CO via *Firmicutes*.

Our study presents novel insights demonstrating how temperature shapes microbial community structure and metabolic pathways in continuously operated biomethanation bioreactors under varying  $H_2$

syngas compositions. Thus, previous studies have explored the temperature effect on microbial community enrichment and metabolic pathways in batch cultures for syngas biomethanation (inherently with a low gas supply and with a limited number of generations). However, this work provided a comprehensive characterization of microbial dynamics during continuous enrichment under mesophilic and thermophilic conditions, which enhances our understanding of microbial interactions in configurations that more accurately represent actual biomethanation processes, facilitating the optimization and tailoring of future systems for industrial applications.

#### 4. Conclusion

This study successfully enriched robust microbial communities for the conversion of syngas into  $\text{CH}_4$  during the long-term operation of BCBs under mesophilic and thermophilic conditions. Syngas was converted into  $\text{CH}_4$  via the direct hydrogenotrophic and indirect acetoclastic and carboxydrotrophic pathways under mesophilic conditions, and exclusively via the direct hydrogenotrophic and indirect carboxydrotrophic hydrogenogenesis pathways under thermophilic conditions. By correlating trophic groups with specific microbial taxa, this study provided novel insights into the role of temperature as a critical factor influencing metabolic interactions, as well as its impact on the abundance of specific microorganisms and the overall performance of the biomethanation process across varying syngas compositions in continuously operated enrichment systems. These findings provide practical guidance for selecting operational temperatures based on desired microbial activity, supporting the tailored design of syngas biomethanation systems for industrial applications. Future work should focus on determining and improving gas-liquid mass transfer rates and optimizing biomethanation performance at larger scales.

#### CRediT authorship contribution statement

**Víctor Rodríguez-Gallego:** Writing – original draft, Methodology, Investigation, Formal analysis. **Paula Bucci:** Writing – review & editing, Investigation. **Raquel Lebrero:** Writing – review & editing, Validation, Funding acquisition. **Raúl Muñoz:** Writing – review & editing, Validation, Supervision, Resources, Funding acquisition, Data curation, Conceptualization.

#### Declaration of competing interest

The authors declare that they have no known competing financial interests or personal relationships that could have appeared to influence the work reported in this paper.

#### Acknowledgments

This research was funded by the Spanish Ministry of Science and Innovation (PLEC2022-009349 and PID2021-124347OB-I00). The financial support from the Regional Government of Castilla y León (JCyL) and the FEDER program (UIC379 and UIC393) are also gratefully acknowledged. The authors would like to thank E. Marcos and A. Crespo for their practical support during VFAs, GC and TS/VS analyses.

#### Appendix A. Supplementary data

Supplementary data to this article can be found online at <https://doi.org/10.1016/j.biortech.2025.133082>.

#### Data availability

Data will be made available on request.

#### References

Andreides, D., Bautista Quispe, J.I., Bartackova, J., Pokorna, D., Zabranska, J., 2021. A novel two-stage process for biological conversion of syngas to biomethane. *Biore sour. Technol.* 327, 124811. <https://doi.org/10.1016/j.biortech.2021.124811>.

Arantes, A.L., Alves, J.I., Stams, A.J.M., Alves, M.M., Sousa, D.Z., 2018. Enrichment of syngas-converting communities from a multi-orifice baffled bioreactor. *J. Microbiol. Biotechnol.* 11, 639–646. <https://doi.org/10.1111/1751-7915.12864>.

Arantes, A.L., Moreira, J.P.C., Diender, M., Parshina, S.N., Stams, A.J.M., Alves, M.M., Alves, J.I., Sousa, D.Z., 2020. Enrichment of Anaerobic Syngas-Converting Communities and Isolation of a Novel Carboxydrotrophic *Acetobacterium wieringae* Strain JM. *Front. Microbiol.* 11, 58. <https://doi.org/10.3389/fmicb.2020.00058>.

Asimakopoulos, K., Gavala, H.N., Skiadas, I.V., 2020a. Biomethanation of Syngas by Enriched mixed Anaerobic Consortia in Trickle Bed Reactors. *Waste Biomass Valoriz.* 11, 495–512. <https://doi.org/10.1007/s12649-019-00649-2>.

Asimakopoulos, K., Gavala, H.N., Skiadas, I.V., 2018. Reactor systems for syngas fermentation processes: a review. *Chem. Eng. J.* 348, 732–744. <https://doi.org/10.1016/j.cej.2018.05.003>.

Asimakopoulos, K., Grimalt-Alemany, A., Lundholm-Höffner, C., Gavala, H.N., Skiadas, I.V., 2021a. Carbon Sequestration through Syngas Biomethanation coupled with  $\text{H}_2$  Supply for a Clean production of Natural Gas Grade Biomethane. *Waste Biomass Valoriz.* 12, 6005–6019. <https://doi.org/10.1007/s12649-021-01393-2>.

Asimakopoulos, K., Kaufmann-Elfang, M., Lundholm-Höffner, C., Rasmussen, N.B.K., Grimalt-Alemany, A., Gavala, H.N., Skiadas, I.V., 2021b. Scale up study of a thermophilic trickle bed reactor performing syngas biomethanation. *Appl. Energy* 290, 116771. <https://doi.org/10.1016/j.apenergy.2021.116771>.

Asimakopoulos, K., Łęzyk, M., Grimalt-Alemany, A., Melas, A., Wen, Z., Gavala, H.N., Skiadas, I.V., 2020b. Temperature Effects on Syngas Biomethanation Performed in a Trickle Bed Reactor. *Chem. Eng. J.* 393. <https://doi.org/10.1016/j.cej.2020.124739>.

Biderer-Petit, C., Mbarki, M., Courtine, D., Benarab, Y., Vial, C., Fontanille, P., Dubessay, P., Keramati, M., Jouan-Dufournel, I., Monjot, A., Guez, J.S., Fadhlouai, K., 2024. Comparison of methane yield of a novel strain of *Methanothermobacter marburgensis* in pure and mixed adapted culture derived from a methanation bubble column bioreactor. *Biore sour. Technol.* 406, 131021. <https://doi.org/10.1016/j.biortech.2024.131021>.

Bovio-Winkler, P., Guerrero, L.D., Erijman, L., Oyarzúa, P., Suárez-Ojeda, M.E., Cabezas, A., Etcheberere, C., 2023. Genome-centric metagenomic insights into the role of *Chloroflexi* in anammox, activated sludge and methanogenic reactors. *BMC Microbiol.* 23, 45. <https://doi.org/10.1186/s12866-023-02765-5>.

Bridgewater, L.L., Baird, R.B., Eaton, A.D., Rice, E.W., Association, A.P.H., Association, A.W.W., Federation, W.E. (Eds.), 2017. *Standard Methods for the Examination of Water and Wastewater*, 23rd, edition. ed. American Public Health Association, Washington, DC.

Calero, M., Godoy, V., Heras, C.G., Lozano, E., Arjandas, S., Martín-Lara, M.A., 2023. Current state of biogas and biomethane production and its implications for Spain. *Sustain. Energy Fuels* 7, 3584–3602. <https://doi.org/10.1039/D3SE00419H>.

Chen, X., Cui, Z., Zhao, Y., Zhu, N., Liu, Y., Hu, Z., Yuan, X., 2024. Synergistic mechanism of substrate hydrolysis and methanogenesis under “gradient anaerobic digestion” process. *Energy Convers. Manag.* 309, 118443. <https://doi.org/10.1016/j.enconman.2024.118443>.

Cheng, G., Gabler, F., Pizzul, L., Olsson, H., Nordberg, Å., Schnürer, A., 2022. Microbial community development during syngas methanation in a trickle bed reactor with various nutrient sources. *Appl. Microbiol. Biotechnol.* 106, 5317–5333. <https://doi.org/10.1007/s00253-022-12035-5>.

Dyksma, S., Jansen, L., Gallert, C., 2020. Syntrophic acetate oxidation replaces acetoclastic methanogenesis during thermophilic digestion of biowaste. *Microbiome* 8, 105. <https://doi.org/10.1186/s40168-020-00862-5>.

European Biogas Association, 2023. European Biogas Statistical Report 2023. December 2023. Available from: <https://www.europeanbiogas.eu/eba-statistical-report-2023/> (accessed 26 June 2024).

Figueras, J., Benbelkacem, H., Dumas, C., Buffiere, P., 2021. Biomethanation of syngas by enriched mixed anaerobic consortium in pressurized agitated column. *Biore sour. Technol.* 338, 125548. <https://doi.org/10.1016/j.biortech.2021.125548>.

García-Casado, S., Muñoz, R., Lebrero, R., 2024. Enrichment of a mixed syngas-converting culture for volatile fatty acids and methane production. *Biore sour. Technol.* 400, 130646. <https://doi.org/10.1016/j.biortech.2024.130646>.

Gavala, H.N., Skiadas, I.V., 2025. Operation at thermophilic temperatures: an underestimated asset for gas fermentation processes. *Curr. Opin. Biotechnol.* 94, 103319. <https://doi.org/10.1016/j.copbio.2025.103319>.

Goonsekera, E.M., Grimalt-Alemany, A., Thanasoula, E., Yousif, H.F., Krarup, S.L., Valerin, M.C., Angelidakis, I., 2024. Biofilm mass transfer and thermodynamic constraints shape biofilm in trickle bed reactor syngas biomethanation. *Chem. Eng. J.* 500, 156629. <https://doi.org/10.1016/j.cej.2024.156629>.

Grimalt-Alemany, A., Asimakopoulos, K., Skiadas, I.V., Gavala, H.N., 2020a. Modeling of syngas biomethanation and catabolic route control in mesophilic and thermophilic mixed microbial consortia. *Appl. Energy* 262, 114502. <https://doi.org/10.1016/j.apenergy.2020.114502>.

Grimalt-Alemany, A., Łęzyk, M., Kennes-Veiga, D.M., Skiadas, I.V., Gavala, H.N., 2020b. Enrichment of Mesophilic and Thermophilic mixed Microbial Consortia for Syngas Biomethanation: the Role of Kinetic and Thermodynamic Competition. *Waste Biomass Valoriz.* 11, 465–481. <https://doi.org/10.1007/s12649-019-00595-z>.

Grimalt-Alemany, A., Skiadas, I.V., Gavala, H.N., 2018. Syngas biomethanation: state-of-the-art review and perspectives. *Biofuels Bioprod. Biorefining* 12, 139–158. <https://doi.org/10.1002/bbb.1826>.

Hattori, S., 2008. Syntrophic Acetate-Oxidizing Microbes in Methanogenic Environments. *Microbes Environ.* 23, 118–127. <https://doi.org/10.1264/jsme2.23.118>.

Henstra, A.M., Sipma, J., Rinzema, A., Stams, A.J., 2007. Microbiology of synthesis gas fermentation for biofuel production. *Curr. Opin. Biotechnol.* 18, 200–206. <https://doi.org/10.1016/j.copbio.2007.03.008>.

Holmes, D.E., Smith, J.A., 2016. Biologically Produced Methane as a Renewable Energy Source, in: *Advances in Applied Microbiology*. Elsevier, pp. 1–61. <https://doi.org/10.1016/bs.aambs.2016.09.001>.

Hu, X., Jiang, B., Yu, C., Söderlind, U., Göransson, K., Zhang, W., 2024. Product gas biomethanation with inoculum enrichment and grinding. *Biomass Convers. Biorefinery* 14, 12993–13004. <https://doi.org/10.1007/s13399-022-03490-1>.

Jarrell, K.F., 1985. Extreme Oxygen Sensitivity in Methanogenic Archaeabacteria. *Bioscience* 35, 298–302. <https://doi.org/10.2307/1309929>.

Jiang, B., Zhang, D., Hu, X., Söderlind, U., Paladino, G., Gamage, S., Hedenstrom, E., Zhang, W., Arrigoni, J., Lundgren, A., Tuveson, M., Yu, C., 2023. Low-Grade Syngas Biomethanation in Continuous Reactors with respect to Gas–Liquid Mass transfer and Reactor Start-up strategy. *Fermentation* 9, 38. <https://doi.org/10.3390/fermentation9010038>.

Kato, M.T., Field, J.A., Lettinga, G., 1993. High tolerance of methanogens in granular sludge to oxygen. *Biotechnol. Bioeng.* 42, 1360–1366. <https://doi.org/10.1002/bit.260421113>.

Keramati, M., Erdogan, K., Guez, J.-S., Ursu, A.V., Dubessay, P., Vial, C., Fontanille, P., 2024. Intensification of ex-situ biomethanation in a bubble column bioreactor by addition of colonized biochips. *Bioresour. Technol. Rep.* 27, 101938. <https://doi.org/10.1016/j.biteb.2024.101938>.

Kuipers, S.B., Kofoed, M.V.W., 2023. Biomethanation of syngas in packed bed reactors: a study of adaptation and microbial pathways in a thermophilic mixed consortium. *Bioresour. Technol. Rep.* 24, 101667. <https://doi.org/10.1016/j.biteb.2023.101667>.

Laguillaumie, L., Raftari, Y., Moya-Leclair, E., Delagnes, D., Dubos, S., Spérandio, M., Paul, E., Dumas, C., 2022. Stability of ex situ biological methanation of H<sub>2</sub>/CO<sub>2</sub> with a mixed microbial culture in a pilot scale bubble column reactor. *Bioresour. Technol.* 354, 127180. <https://doi.org/10.1016/j.biortech.2022.127180>.

Latif, H., Zeidan, A.A., Nielsen, A.T., Zengler, K., 2014. Trash to treasure: production of biofuels and commodity chemicals via syngas fermenting microorganisms. *Curr. Opin. Biotechnol.* 27, 79–87. <https://doi.org/10.1016/j.copbio.2013.12.001>.

Li, C., Zhu, X., Angelidaki, I., 2021. Syngas biomethanation: effect of biomass-gas ratio, syngas composition and pH buffer. *Bioresour. Technol.* 342, 125997. <https://doi.org/10.1016/j.biortech.2021.125997>.

Li, C., Zhu, X., 2020. Carbon monoxide conversion and syngas biomethanation mediated by different microbial consortia. *Bioresour. Technol.* 314, 123739. <https://doi.org/10.1016/j.biortech.2020.123739>.

Li, Y., Liu, Y., Wang, X., Luo, S., Su, D., Jiang, H., Zhou, H., Pan, J., Feng, L., 2022. Biomethanation of syngas at high CO concentration in a continuous mode. *Bioresour. Technol.* 346, 126407. <https://doi.org/10.1016/j.biortech.2021.126407>.

Li, C., Luo, G., Wang, W., He, Y., Zhang, R., Liu, G., 2018. The effects of pH and temperature on the acetate production and microbial community compositions by syngas fermentation. *Fuel* 224, 537–544. <https://doi.org/10.1016/j.fuel.2018.03.125>.

Liu, R., Hao, X., Wei, J., 2016. Function of homoacetogenesis on the heterotrophic methane production with exogenous H<sub>2</sub>/CO<sub>2</sub> involved. *Chem. Eng. J.* 284, 1196–1203. <https://doi.org/10.1016/j.cej.2015.09.081>.

Luo, G., Angelidaki, I., 2013. Hollow fiber membrane based H<sub>2</sub> diffusion for efficient in situ biogas upgrading in an anaerobic reactor. *Appl. Microbiol. Biotechnol.* 97, 3739–3744. <https://doi.org/10.1007/s00253-013-4811-3>.

Magoć, T., Salzberg, S.L., 2011. FLASH: fast length adjustment of short reads to improve genome assemblies. *Bioinformatics* 27, 2957–2963. <https://doi.org/10.1093/bioinformatics/btr507>.

Meegoda, J.N., Li, B., Patel, K., Wang, L.B., 2018. A Review of the Processes, Parameters, and Optimization of Anaerobic Digestion. *Int. J. Environ. Res. Public Health* 15, 2224. <https://doi.org/10.3390/ijerph15102224>.

Mignogna, D., Ceci, P., Cafaro, C., Corazza, G., Avino, P., 2023. Production of Biogas and Biomethane as Renewable Energy sources: a Review. *Appl. Sci.* 13, 10219. <https://doi.org/10.3390/app131810219>.

Morgan-Sagastume, F., Jacobsson, S., Olsson, L.E., Carlsson, M., Gyllenhammar, M., Sárvári Horváth, I., 2019. Anaerobic treatment of oil-contaminated wastewater with methane production using anaerobic moving bed biofilm reactors. *Water Res.* 163, 114851. <https://doi.org/10.1016/j.watres.2019.07.018>.

Muyzer, G., Teske, A., Wirsén, C.O., Jannasch, H.W., 1995. Phylogenetic relationships of *Thiamicospira* species and their identification in deep-sea hydrothermal vent samples by denaturing gradient gel electrophoresis of 16S rDNA fragments. *Arch. Microbiol.* 164, 165–172. <https://doi.org/10.1007/BF02529967>.

Navarro, S.S., Cimpoia, R., Bruant, G., Guiot, S.R., 2014. Specific inhibitors for identifying pathways for methane production from carbon monoxide by a nonadapted anaerobic mixed culture. *Can. J. Microbiol.* 60, 407–415. <https://doi.org/10.1139/cjm-2013-0843>.

Omae, K., Fukuyama, Y., Yasuda, H., Mise, K., Yoshida, T., Sako, Y., 2019. Diversity and distribution of thermophilic hydrogenogenic carboxydrotrophs revealed by microbial community analysis in sediments from multiple hydrothermal environments in Japan. *Arch. Microbiol.* 201, 969–982. <https://doi.org/10.1007/s00203-019-01661-9>.

Palacios, P.A., Sieborg, M.U., Kuipers, S.B., Fruergaard, S., Kofoed, M.V.W., 2025. Temperature tactics: Targeting acetate or methane production in autotrophic H<sub>2</sub>/CO<sub>2</sub> conversion with mixed cultures. *Biochem. Eng. J.* 214, 109574. <https://doi.org/10.1016/j.bej.2024.109574>.

Pan, X., Zhao, L., Li, C., Angelidaki, I., Lv, N., Ning, J., Cai, G., Zhu, G., 2021. Deep insights into the network of acetate metabolism in anaerobic digestion: focusing on syntrophic acetate oxidation and homoacetogenesis. *Water Res.* 190, 116774. <https://doi.org/10.1016/j.watres.2020.116774>.

Paniagua, S., Lebrero, R., Muñoz, R., 2022. Syngas biomethanation: current state and future perspectives. *Bioresour. Technol.* 358, 127436. <https://doi.org/10.1016/j.biortech.2022.127436>.

Parada, A.E., Needham, D.M., Fuhrman, J.A., 2016. Every base matters: assessing small subunit rRNA primers for marine microbiomes with mock communities, time series and global field samples. *Environ. Microbiol.* 18, 1403–1414. <https://doi.org/10.1111/1462-2920.13023>.

Quast, C., Pruesse, E., Yilmaz, P., Gerken, J., Schweer, T., Yarza, P., Peplies, J., Glöckner, F.O., 2012. The SILVA ribosomal RNA gene database project: improved data processing and web-based tools. *Nucleic Acids Res.* 41, D590–D596. <https://doi.org/10.1093/nar/gks1219>.

Raftari, Y., Laguillaumie, L., Dumas, C., 2021. Biological Methanation of H<sub>2</sub> and CO<sub>2</sub> with mixed Cultures: current advances, Hurdles and challenges. *Waste Biomass Valoriz.* 12, 5259–5282. <https://doi.org/10.1007/s12649-020-01283-z>.

Ross, D.E., Marshall, C.W., Gulliver, D., May, H.D., Norman, R.S., 2020. Defining Genomic and Predicted Metabolic Features of the *Acetobacterium*. *Genus mSystems* 5, e00277–e00320. <https://doi.org/10.1128/mSystems.00277-20>.

Sancho Navarro, S., Cimpoia, R., Bruant, G., Guiot, S.R., 2016. Biomethanation of Syngas using Anaerobic Sludge: Shift in the Catabolic Routes with the CO Partial pressure increase. *Front. Microbiol.* 7. <https://doi.org/10.3389/fmicb.2016.01188>.

Sieborg, M.U., Engelbrecht, N., Singh, A., Schnürer, A., Ottosen, L.D.M., Kofoed, M.V.W., 2025. Unraveling the effects of temperature on mass transfer and microbiology in thermophilic and extreme thermophilic trickle bed biomethanation reactors. *Chem. Eng. J.* 509, 161179. <https://doi.org/10.1016/j.cej.2025.161179>.

Sousa, D.Z., Smidt, H., Alves, M.M., Stams, A.J.M., 2007. *Syntrophomonas zehnderi* sp. nov., an anaerobe that degrades long-chain fatty acids in co-culture with *Methanobacterium formicum*. *Int. J. Syst. Evol. Microbiol.* 57, 609–615. <https://doi.org/10.1099/ijss.0.64734-0>.

Sposób, M., 2024. Optimization of ex-situ biomethanation process in trickle bed reactor: the impact of slight H<sub>2</sub>/CO<sub>2</sub> ratio adjustments and different packing materials. *Renew. Energy* 222, 119971. <https://doi.org/10.1016/j.renene.2024.119971>.

Spiridonidis, A., Vasilidiou, I.A., Stathopoulou, P., Tsiamis, A., Tsiamis, G., Stamatelatou, K., 2023. Enrichment of Microbial Consortium with Hydrogenotrophic Methanogens for Biological Biogas Upgrade to Biomethane in a Bubble Reactor under Mesophilic Conditions. *Sustainability* 15, 15247. <https://doi.org/10.3390/su152115247>.

Thapa, A., Park, J.-G., Jun, H.-B., 2022. Enhanced ex-situ biomethanation of hydrogen and carbon dioxide in a trickling filter bed reactor. *Biochem. Eng. J.* 179, 108311. <https://doi.org/10.1016/j.bej.2021.108311>.

Tsapekos, P., Alvarado-Morales, M., Angelidaki, I., 2022. H<sub>2</sub> competition between homoacetogenic bacteria and methanogenic archaea during biomethanation from a combined experimental-modelling approach. *J. Environ. Chem. Eng.* 10, 107281. <https://doi.org/10.1016/j.jece.2022.107281>.

Tunca, B., Rovithi, A., Dutta, S., Quintela, C., Pinelo, M., Skiadas, I.V., Gavala, H.N., 2025. Enhanced Carbon Monoxide Bioconversion through Adaptation of mixed Microbial Consortia in Trickle Bed Reactors. *Waste Biomass Valoriz.* <https://doi.org/10.1007/s12649-025-02945-6>.

Westman, S., Chandolias, K., Taherzadeh, M., 2016. Syngas Biomethanation in a Semi-Continuous reverse Membrane Bioreactor (RMBR). *Fermentation* 2, 8. <https://doi.org/10.3390/fermentation20008>.

Wu, S.C., Liou, S.Z., Lee, C.M., 2012. Correlation between bio-hydrogen production and polyhydroxybutyrate (PHB) synthesis by *Rhodopseudomonas palustris* WP3-5. *Bioresour. Technol.* 113, 44–50. <https://doi.org/10.1016/j.biortech.2012.01.090>.

Xu, J., Bu, F., Zhu, W., Luo, G., Xie, L., 2020. Microbial Consortiums of Hydrogenotrophic Methanogenic mixed Cultures in Lab-Scale Ex-Situ Biogas Upgrading Systems under Different Conditions of Temperature, pH and CO. *Microorganisms* 8, 772. <https://doi.org/10.3390/microorganisms8050772>.

Yun, Y.-M., Sung, S., Kang, S., Kim, M.-S., Kim, D.-H., 2017. Enrichment of hydrogenotrophic methanogens by means of gas recycle and its application in biogas upgrading. *Energy* 135, 294–302. <https://doi.org/10.1016/j.energy.2017.06.133>.

Zeng, Y., Zheng, D., Li, L.-P., Wang, M., Gou, M., Kamagata, Y., Chen, Y.-T., Nobu, M.K., Tang, Y.-Q., 2024. Metabolism of novel potential syntrophic acetate-oxidizing bacteria in thermophilic methanogenic chemostats. *Appl. Environ. Microbiol.* 90. <https://doi.org/10.1128/aem.01090-23>.

Zheng, D., Wang, H.-Z., Gou, M., Nobu, M.K., Narihiro, T., Hu, B., Nie, Y., Tang, Y.-Q., 2019. Identification of novel potential acetate-oxidizing bacteria in thermophilic methanogenic chemostats by DNA stable isotope probing. *Appl. Microbiol. Biotechnol.* 103, 8631–8645. <https://doi.org/10.1007/s00253-019-10078-9>.

Zheng, X., Zhou, W., Min, B., Zhou, Y., Xie, L., 2023. Impact of carbon monoxide on performance and microbial community of extreme-thermophilic hydrogenotrophic methanation in horizontal rotary bioreactor. *Bioresour. Technol.* 384, 129248. <https://doi.org/10.1016/j.biortech.2023.129248>.